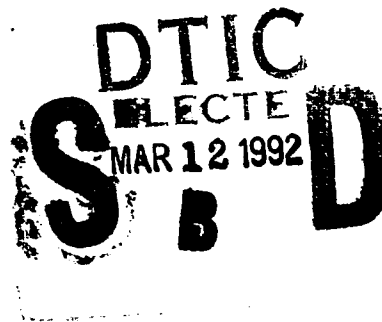


AD-A247 916



2

A Probabilistic Neural Network Approach to Cloud Classification



R. L. Bankert
Prediction Systems Division
Atmospheric Directorate
Monterey, CA 93943-5006

P. Rabindra
S. K. Sengupta
University Corporation for Atmospheric Research
Boulder, CO 80307-3000



Approved for public release; distribution is unlimited. Naval
Oceanographic and Atmospheric Research Laboratory, Stennis Space
Center, Mississippi 39529-5004.

92-06219



82 3 00 157

ABSTRACT

Automated satellite image interpretation would be useful in many forecasting operations. One aspect of that interpretation, cloud classification, is examined. Ten classes, composed of low, middle, high, and precipitation cloud types plus clear, are used as output nodes in a Probabilistic Neural Network (PNN) approach to classification of data using four Advanced Very High Resolution Radiometer (AVHRR) subscenes. Input to the neural network consists of 12 features that include a mixture of spectral, textural, and physical measures. These measures are selected, using a feature selection routine, from a collection of over 200 features. An overall accuracy of 85.15% is the result. Four classes have agreement of 90% or better. The two classes with the poorest accuracies were presented to the classifier with the smallest sample sizes. An increase in the number of samples should increase the accuracy of the classifier.

ACKNOWLEDGMENTS

The authors gratefully acknowledge the support of the sponsor, Office of Naval Technology, Code 22, Mr. James Cauffman, Program Element 62435N, for making this effort possible.

The overall guidance and supervision of this project by Dr. Paul Tag of NOARL is also acknowledged. Finally, the authors gratefully acknowledge the contributions of the Naval Postgraduate School and, in particular, Professors Carlyle Wash and Forrest Williams for their careful analysis of the data necessary to make this research effort possible.

TABLE OF CONTENTS

1. Introduction.....	1
2. Background.....	2
3. Data Description.....	8
4. Data Processing Procedures.....	9
5. Results.....	19
6. Summary.....	22
References.....	26

Accession For	
NTIS GRA&I	<input checked="" type="checkbox"/>
DTIC TAB	<input type="checkbox"/>
Unannounced	<input type="checkbox"/>
Justification	
By _____	
Distribution/	
Availability Codes	
Dist	Avail and/or Special
A-1	

A Probabilistic Neural Network Approach to Cloud Classification

1. Introduction

High quality real-time satellite imagery would provide valuable information to any shipboard forecaster. With the advent of the proper shipboard equipment, this additional forecasting assistance will soon be available. Unfortunately, detailed imagery interpretation is a talent currently limited to a very few experts. Automatic interpretation would ease the burden that would be required of shipboard forecasters to learn, practice, and use this additional skill. With time being a constraining element in any forecasting situation, receiving quickly produced output that could be immediately used as a forecasting or observation tool would be a tremendous asset.

Cloud classification of the pixel data could be a part of the image analysis process. This classification can then be used, for example, as input into a more generalized synoptic analysis of the image or as relevant information to any naval operation. In polar regions, separation of image elements into ice, snow, water, and clouds would be extremely useful. This is true not only in operations, but in climate research as well. Successful validation of the classification methodology employed here was performed earlier on polar data using a unique set of classes (Sengupta et al., 1991). The purpose of this study is to

evaluate the effectiveness of a neural network approach to cloud classification in nonpolar regions.

Based upon the cloud classification procedure developed for the Tactical Environmental Support System (TESS) (Crosiar et al., 1990), twelve classes were established as the output nodes in the neural network. These classes are listed in Table 1. Pixel data from the images were made up of calibrated gray levels (0-255). Input data for the network were gathered from spectral, textural, and physical features computed from the pixel data.

A background of the neural network and input features is provided in section 2. A description of the data is found in section 3. Data processing procedures are found in section 4. A discussion of the results comprises section 5. A summary and future considerations are presented in section 6.

2. Background

Using neural networks to classify cloud types in satellite imagery has shown recent success (Key et al., 1989; Lee et al., 1990). The investigation performed here employs the Probabilistic Neural Network (PNN) approach to cloud classification. The PNN was chosen over other neural networks because of its speed in training without a sacrifice in accuracy. Sengupta et al. (1991) found the PNN to be superior to the Feed-Forward Back Propagation neural network and the more traditional Stepwise Discriminant Analysis.

Table 1. Twelve classes originally considered for testing.

1. Cirrus (Ci)
2. Cirrocumulus (Cc)
3. Cirrostratus (Cs)
4. Altostratus (As)
5. Nimbostratus (Ns)
6. Stratocumulus (Sc)
7. Stratus (St)
8. Cumulus (Cu)
9. Cumulonimbus (Cb)
10. Clear (Clr)
11. Altocumulus (Ac)
12. Cumulus Congestus (CuC)

The PNN makes use of a Bayesian strategy for classification (Specht, 1990). The Bayes decision rule requires calculation of the probability density function of each class. Unknown probability densities can be estimated using the training samples (normalized to unit length) in a Parzen estimator (Specht, 1990). The estimator is given by:

$$f(\bar{x}) = 1/m_c \cdot 1/(2\pi\sigma^2)^{d/2} \sum_{i=1 \rightarrow m_c} \exp[(Z_i - 1)/\sigma^2]$$

where:

\bar{x} - feature vector of testing sample

m_c - number of training patterns in class c

σ - "smoothing parameter"

d - number of features

$Z_i = \bar{y}_i \cdot \bar{x}$ - the dot product of the i^{th} training (normalized) sample and the testing (normalized) sample, point X in the feature space

\tilde{y}_i - training sample in class c

The "smoothing parameter," σ , can be computed from

$$\sigma^2 = Gm_c^{-F}$$

where F and G can be experimented with interactively in the PNN to find the value of σ^2 that provides the best result. As discussed in Specht (1990) the decision boundaries can range from linear as $\sigma \rightarrow \infty$, to very nonlinear as $\sigma \rightarrow 0$. The PNN configuration for a two-class problem is displayed in Figure 1 (Specht, 1990).

The feature vector, built from 203 components, contains spectral, textural, and physical parts. A mixture of component types has been shown in other examinations (Chen et al., 1989; Ebert, 1987 and 1989; Garand, 1988; Goroch and Welch, 1989; Key, 1990; Lee et al., 1990; Welch et al., 1989; Welch et al., 1990) to provide better results than the use of a single type. Textural measures, representing the spatial distribution of gray levels within an image, were calculated using the Gray Level Difference Vector (GLDV) approach and the Sum And Difference Histogram (SADH) method. The following GLDV measures were computed for both channels 1 (0.63 μm) and 4 (10.8 μm) of the AVHRR:

$$\text{mean } \mu = \sum_m mP(m)$$

$$\text{standard deviation } \sigma = [\sum_m (m-\mu)^2 P(m)]^{1/2}$$

$$\text{angular second moment } \text{asm} = \sum_m [P(m)]^2$$

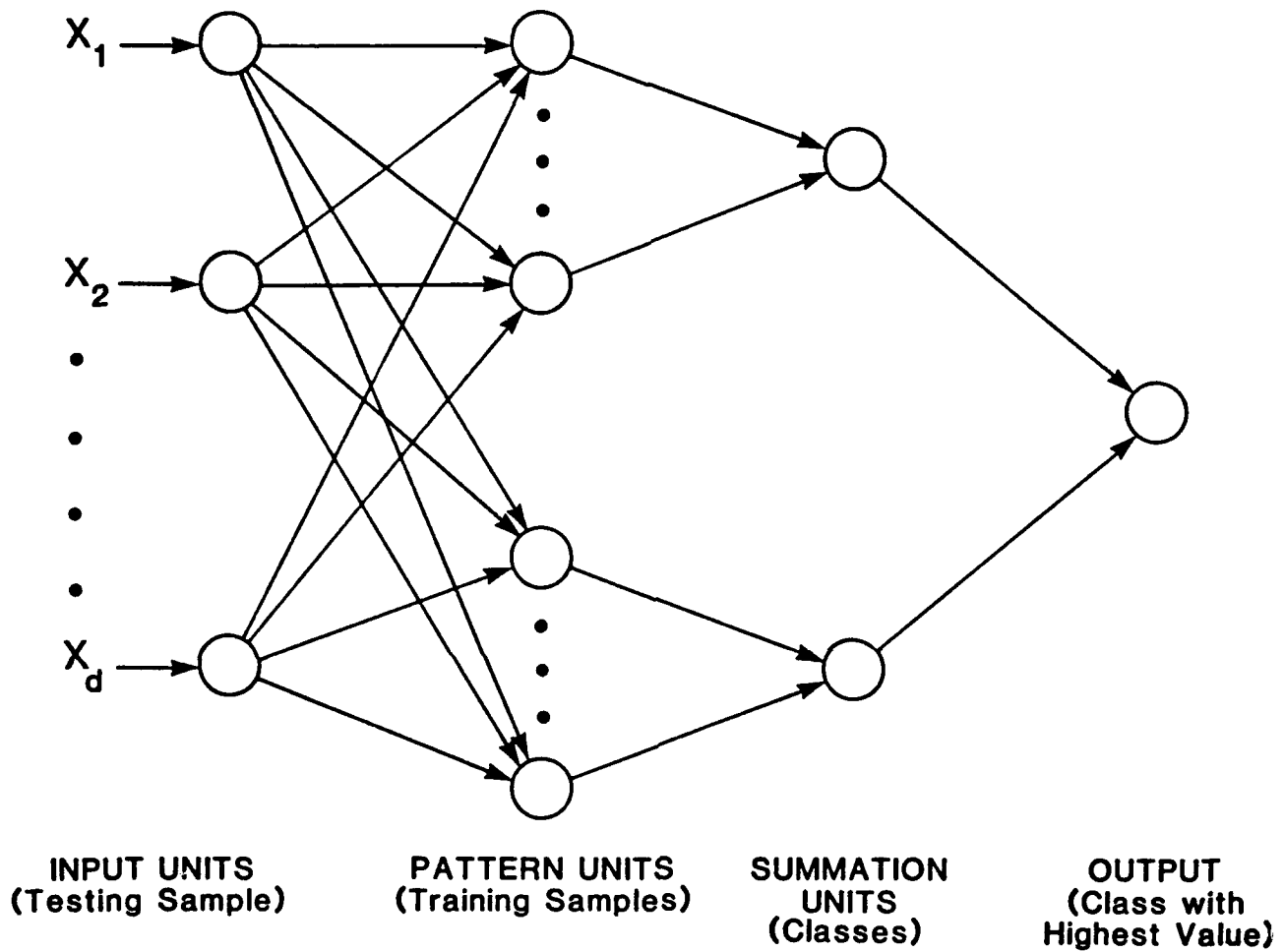


Figure 1. PNN configuration for a two-class problem (adapted from Specht, 1990).

$$\text{entropy } \text{ent} = -\sum_m P(m) \log P(m)$$

$$\text{local homogeneity } \text{lh} = \sum_m P(m) / (1+m^2)$$

$$\text{contrast } \text{con} = \sum_m m^2 P(m)$$

$$\text{cluster shade } \text{cs} = [\sum_m (m-\mu)^3 P(m)] / \sigma^3$$

$$\text{cluster prominence } \text{cp} = [\sum_m (m-\mu)^4 P(m)] / \sigma^4 - 3$$

where $m = |I-J|$, the absolute difference of gray levels one pixel apart in a fixed direction. $P(m)$ is the difference vector probability density function (estimated by gray level frequencies of occurrence / total frequencies). The following SADH measures were computed for channels 1 and 4:

$$\text{mean } \mu_S = \sum_K K P_S(K)$$

$$\text{standard deviation } \text{sd} = \{1/2 [\sum_K (K-\mu_S)^2 P_S(K) + \sum_L L^2 P_D(L)]\}^{1/2}$$

$$\text{angular second moment } \text{asm} = \sum_K [P_S(K)]^2 \sum_L [P_D(L)]^2$$

$$\text{contrast } \text{con} = \sum_L L^2 P_D(L)$$

$$\text{correlation } \text{cor} = 1/2 [\sum_K (K-\mu_S)^2 P_S(K) - \sum_L L^2 P_D(L)] / \text{sd}^2$$

$$\text{entropy } \text{ent} = -\sum_K P_S(K) \log(P_S(K)) - \sum_L P_D(L) \log(P_D(L))$$

$$\text{local homogeneity } \text{lh} = \sum_L P_D(L) / (1+L^2)$$

$$\text{cluster shade } \text{cs} = [\sum_K (K-\mu_S)^3 P_S(K)] / \text{sd}^3$$

$$\text{cluster prominence } \text{cp} = [\sum_K (K-\mu_S)^4 P_S(K)] / \text{sd}^4 - 3$$

where $K=I+J$ and $L=I-J$. $P_S(K)$ and $P_D(L)$ are the probability density functions.

Run length statistics (Connors and Harlow, 1980; Haralick, 1979) were computed for channels 1 and 4. These measures are based on sets of adjacent pixels in a particular direction having the same gray level. The following features were used:

$$\text{short run emphasis } sre = 1/T_r \sum_i \sum_j P(i,j)/j^2$$

$$\text{long run emphasis } lre = 1/T_r \sum_i \sum_j j^2 P(i,j)$$

$$\text{gray level distribution } gld = 1/T_r \sum_i [\sum_j P(i,j)]^2$$

$$\text{run length distribution } rld = 1/T_r \sum_j [\sum_i P(i,j)]^2$$

$$\text{run percentages } rp = 1/T_p \sum_i \sum_j P(i,j) = T_r/T_p$$

where:

$$i = 0 \rightarrow N_g - 1$$

$$j = 1 \rightarrow N_r$$

N_g - number of gray levels

N_r - number of runs

T_p - number of image pixels

$$T_r = \sum_i \sum_j P(i,j)$$

$P(i,j)$ - number of occurrences of runs of length j having gray level i

Spectral measures used as part of the feature vector included maximum, minimum, range, mode, median, mean, and standard

deviation of pixel values in channels 1 and 4.

Finally, physical features from Garand (1988) and Goroch and Welch (1989) were added. They included visible cloud fraction, mean albedo of cloudy pixels, surface temperature, cloud top temperature, infrared cloud fraction, low cloud fraction, mid-level cloud fraction, cirrus cloud fraction, and multilayer cloud index.

3. Data Description

An important step in the development of any supervised classifier is accurately labeling (manually classifying) the images to be used as training (and testing) data. To ensure the quality of this procedure, previously labeled AVHRR subscenes were obtained for this study through the Naval Postgraduate School (NPS) (Neu, 1990). Four nonpolar 512x512 pixel images (Table 2) were labeled by two independent experts (Professors C. Wash and F. Williams) for the purpose of evaluating an automated multispectral cloud classifier (Neu, 1990).

Many cloud types are evident in these subscenes (Figures 2-5 (channel 2 is used for display purposes only)) and eleven of these types (plus clear) were used as classes in the labeling done by the experts (see Table 1). The subscenes included one from the tropics (case 1), two from the subtropics (cases 2 and 3), and one from the midlatitudes (case 4). Thin cirrus, low

Table 2. Four subscenes used for validation of classifier (Neu, 1990).

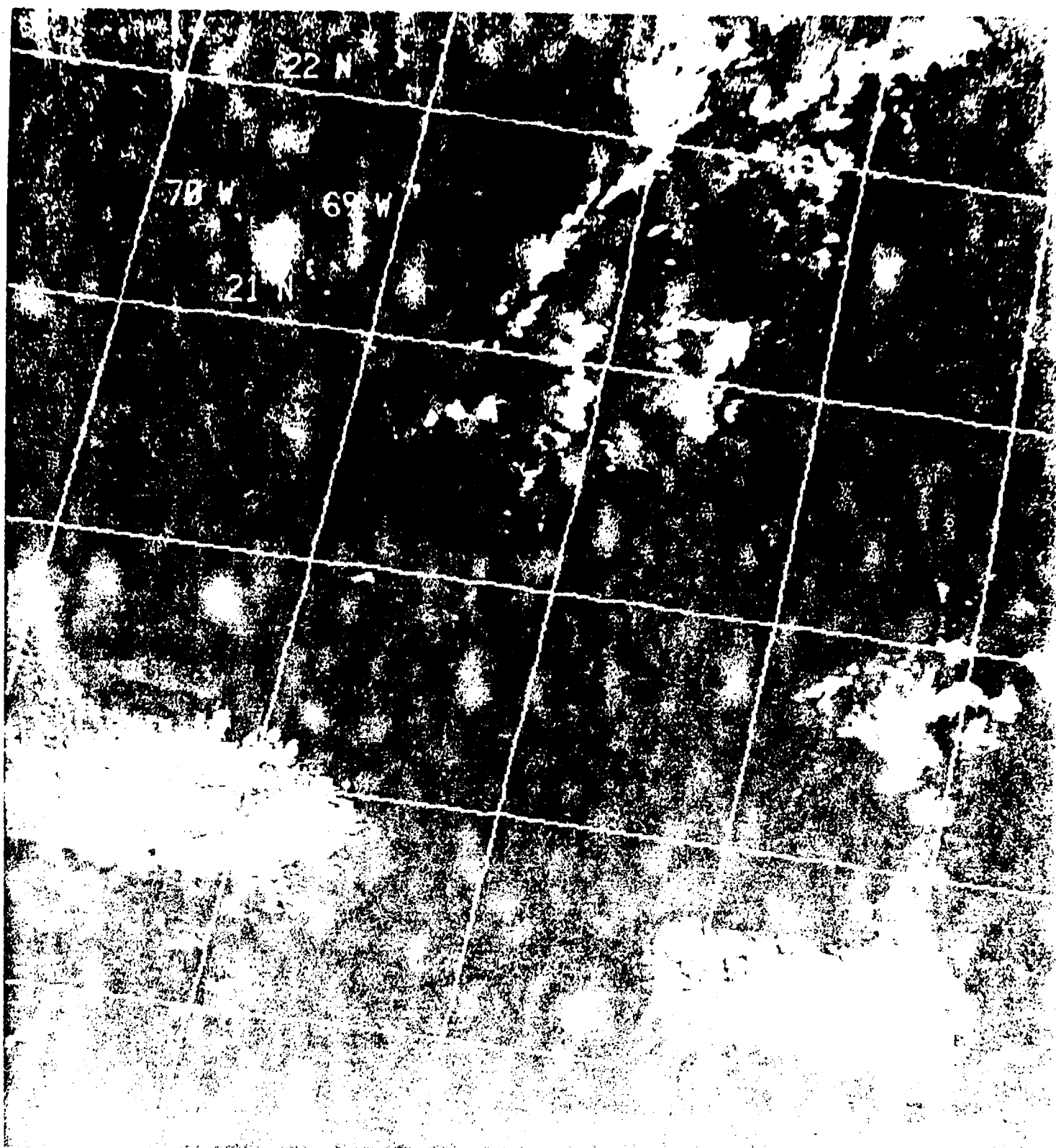
Case	Date	Time (UTC)	Zenith Ang (deg)	Scene Center (deg)	
				Lat. (N)	Lon. (W)
1	13 Dec 88	1809	31.3	20	69
2	17 Jan 88	2256	54.6	34	119
3	13 Dec 88	1809	38.5	34	74
4	14 Dec 88	1758	46.4	42	70

clouds, and developing cumulus are apparent in case 1. An extratropical cyclone in case 2 provides a variety of cloud types including cirrus, convective, stratiform, and cumulus clouds. Case 3 presents an intensifying short wave with various regions of different cloud types. A mixture of low clouds and a band of high clouds make up the midlatitude subscene of case 4.

The experts labeled the subscenes using an 8x8 pixel grid overlay. Only regions for which there was a consensus classification between the experts were considered. This set of labeled data became the foundation for building the collection of samples used in this investigation.

4. Data Processing Procedures

Since calculations of textural measures require larger regions than the 8x8 labeled areas, each 8x8 "box" was examined to determine the feasibility of expanding it to a 32x32 pixel region. With the assistance of Mr. Kim Richardson (NOARL) and Mr. Kurt Nielsen (NPS) the four subscenes were transferred from the



Best Available Copy

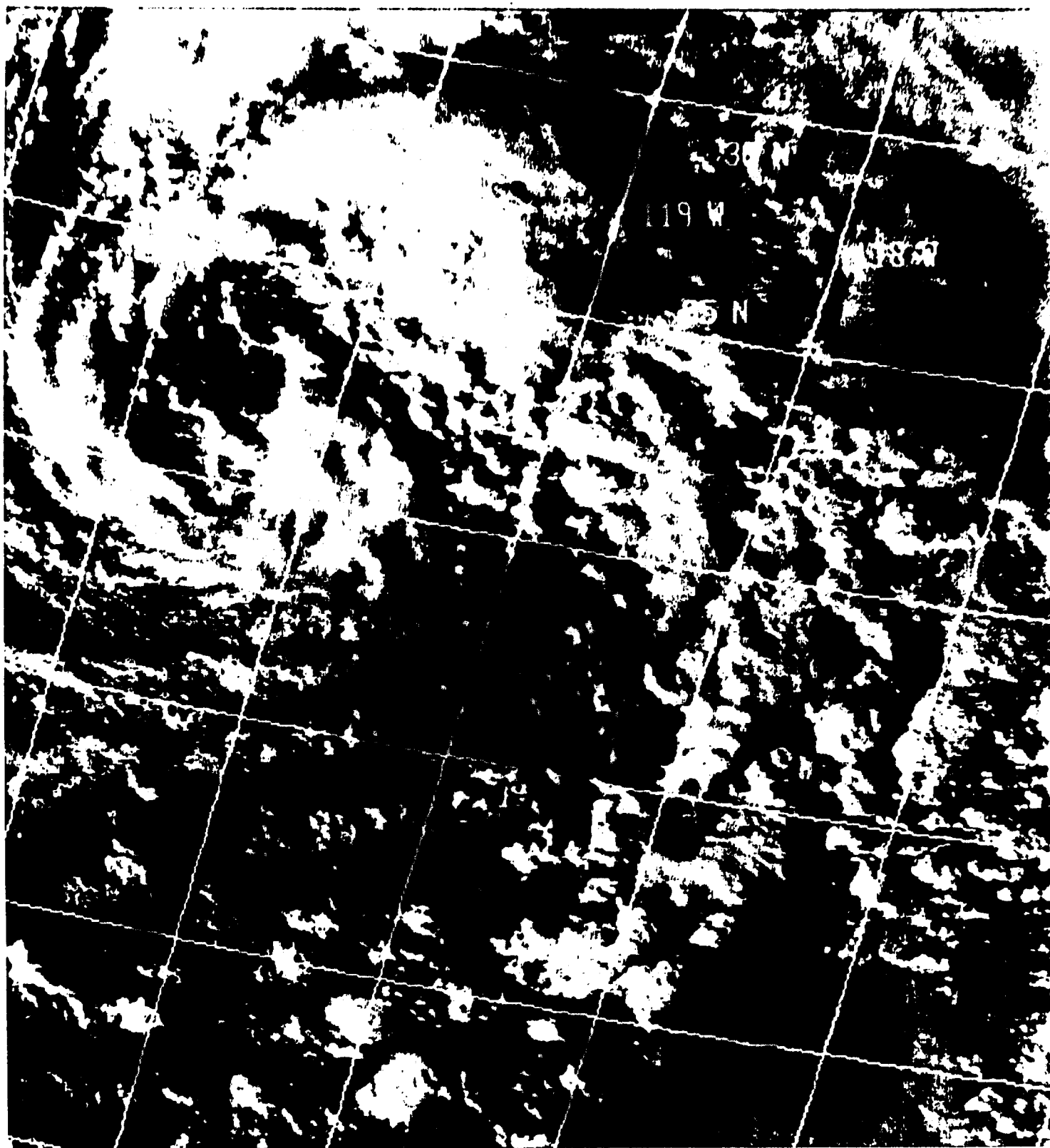


Figure 3. AVHRR channel 2 image of case 2 (see Table 2).

Best Available Copy

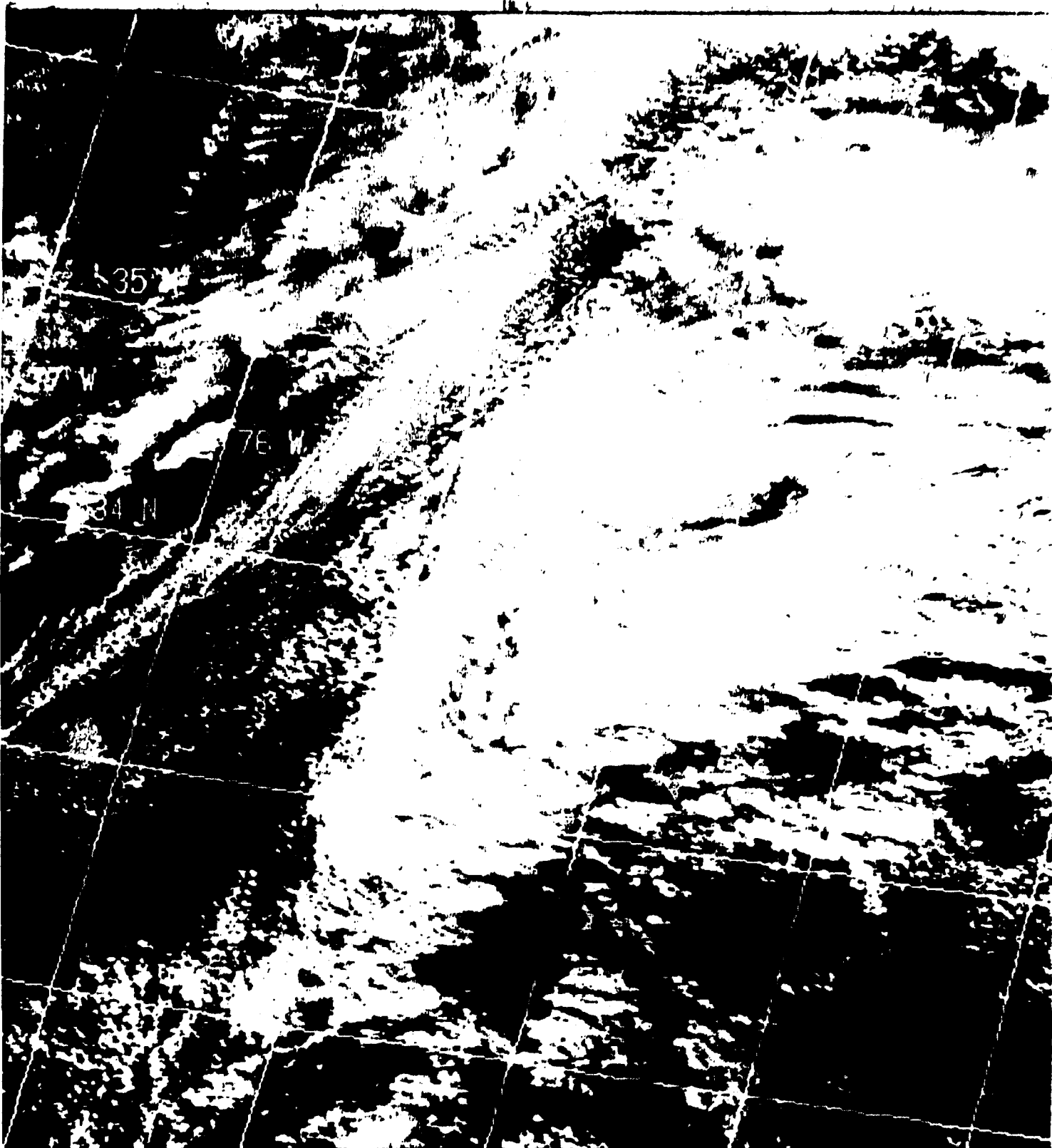
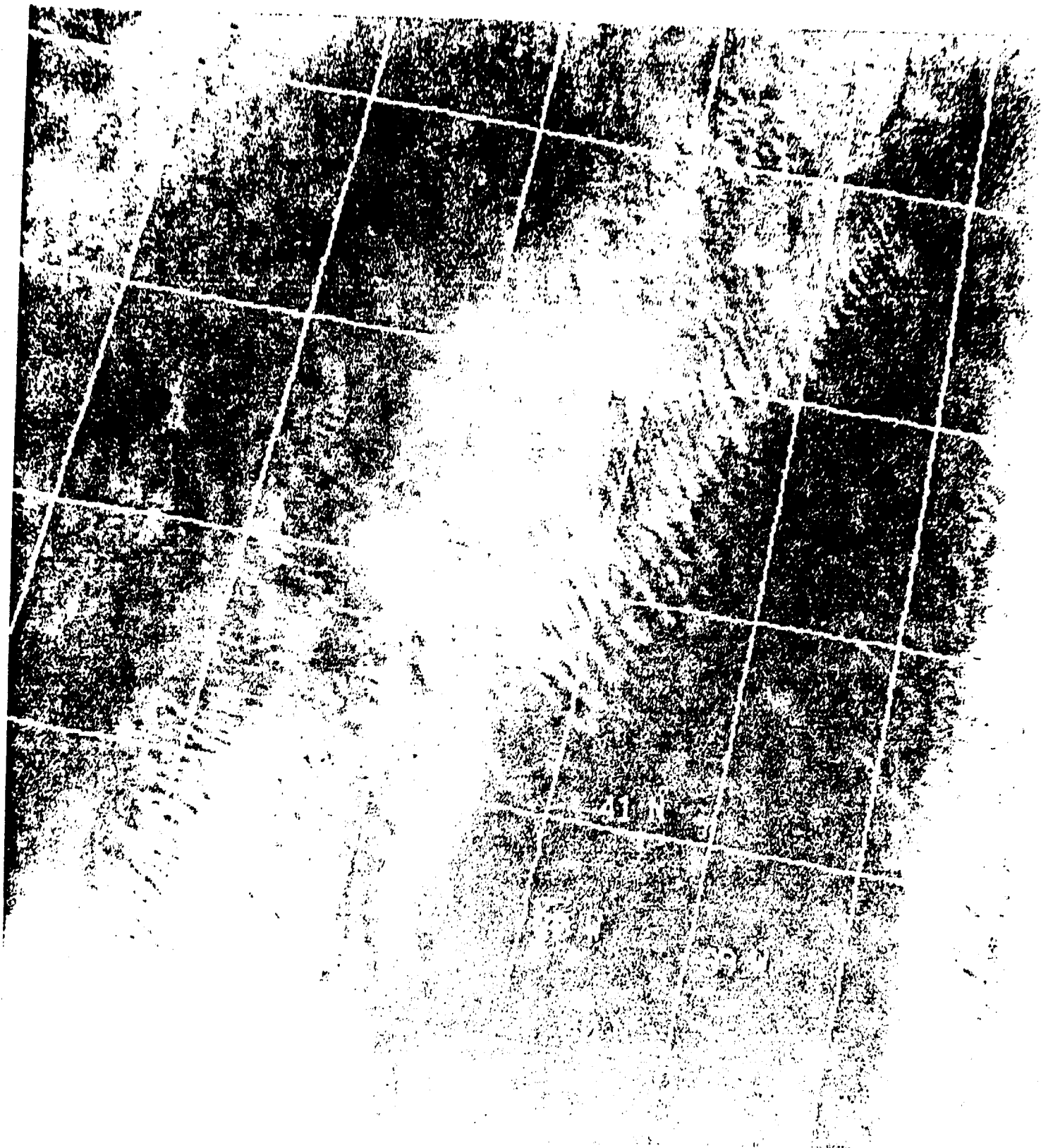


Figure 4. AVHRR channel 2 image of case 3 (see Table 2).



Best Available Copy

NPS computer system to the HP9000/835 Naval Environmental Operational Nowcasting System (NEONS) at NOARL (Jurkevics et al., 1990). Channels 1, 2, and 4, plus a 4-5 difference (channel 4 minus channel 5) were supplied for each subscene. Using the Interactive Data Language (IDL) software package (Research Systems, Inc., 1990), each of the original 187 boxes was examined. Through the use of visual interpretation as well as histogram and statistical comparisons, a total of 105 boxes were expanded to the larger 32x32 region. After discussions among the authors and Dr. Paul Tag of NOARL, more samples were determined to be needed to successfully run the PNN. The subscenes were examined again to find neighboring regions that could be added to the data set. This task resulted in the addition of 67 samples. However, the total of 172 samples was still not of adequate size. A determination was made that a 16x16 pixel region would be a viable alternative and marginally large enough for texture calculations. This decision involved much thought and discussion due to the importance of the calculations of the texture measures. After removing altocumulus and cumulus congestus from the list of classes (too few samples), breaking up the 32x32 size boxes into four separate regions created 668 16x16 samples. From this new set, 610 samples were determined to be useful and formed the final data set. The number of samples for each cloud type that was used to train (2/3 of the samples from each class) and test (1/3 of the samples from each class) the PNN classifier is

displayed in Table 3.

Components of the feature vector for each sample were calculated. These components were comprised of 170 textural measures (GLDV and SADH), 14 spectral measures, and 19 other features (run length statistics and physical measures). Texture calculations were performed on the 16x16 pixel region and each of the 16 4x4 pixel regions within the 16x16 area. The maximum, minimum, mean, and standard deviation of the values from the smaller areas were used as components (along with the 16x16 value) in the feature vector for each texture measure. A complete listing of the measures is presented in Table 4. Subroutines were written in IDL to compute the features for each sample, with the resulting data and class type number written to a file. Each feature was normalized and run through a feature selection routine to determine the order of importance of the features in discriminating the 10 cloud classes. This routine uses the Bhattacharya Class Separability Index and a Sequential Forward Selection method (Devijver and Kittler, 1982). This ranking procedure was an initial step in the reduction of the dimensions of the feature vector so that measures of little or no use to the classification could be removed. The top 50 features, in order of importance, are listed in Table 5.

A rule of thumb suggests that the minimum number of training samples (per class) required for a robust training of the neural

Table 3. Number of training and testing samples in each class.

<u>Class</u>	<u>Training</u>	<u>Testing</u>	<u>Total</u>
Ci	71	35	106
Cc	38	19	57
Cs	25	12	37
As	27	13	40
Ns	40	19	59
Sc	44	21	65
St	58	28	86
Cu	36	18	54
Cb	27	14	41
Clr	44	21	65
Total	410	200	610

network is

(Number of classes + Number of features) x 5.

Using this rule of thumb and given the size of the current data set for each class, more data are needed. However, the data set was considered large enough to obtain a preliminary evaluation and a PNN classification was performed.

A breakdown of the data into training and testing samples was required to determine the accuracy of the classifier. A random selection of 2/3 of the samples in each class was performed to create the training set, and the remaining 1/3 made up the testing set. A program was written to perform the random selection and 10 different data sets (different samples selected as training and testing) were created. Using a variety of data sets provided an indication of the consistency of the classifier in the classification of the data. Next, the optimum number of

Table 4. List of 203 features calculated for each sample.

GLDV* and SADH* (170 Features)

Mean
Standard Deviation
Angular Second Moment
Entropy
Local Homogeneity
Contrast
Cluster Shade
Cluster Prominence
Correlation - SADH only

5 values computed for each measure:
16x16 pixel region; maximum,
minimum, mean, standard deviation
of the 16 4x4 pixel regions
within the 16x16

Run Length* (10)

Short Run Emphasis
Long Run Emphasis
Gray Level Dist'n
Run length Dist'n
Run Percentage

Spectral* (14)

Maximum Pixel Value
Minimum Pixel Value
Range of Pixel Values
Mode of Pixel Values
Median of Pixel Values
Mean of Pixel Values
Standard Dev. of Pixel Values

Physical (9)

IR Cloud Fraction
Low Cloud Fraction
Mid-level Cloud Fraction
Cirrus Cloud Fraction
Multilayer Cloud Index
Cloud Top Temperature
Cloud Albedo
Surface Temperature
Visible Cloud Fraction

* AVHRR Channels 1 and 4

features to use to train and test the PNN was determined. The 10 data sets were run on the PNN with a varying number of features. The top five features (see Table 5) were used first. The resultant average overall accuracy of the test samples of the data sets was 74.70%. Then starting at 10 features and incrementing by one (up to a maximum of 20 features), the PNN was trained and tested on the 10 data sets to find the average

Table 5. Top 50 features (in order of importance) selected by feature selection routine.

1. Cloud albedo
2. SADH angular second moment, channel 4, mean 4x4 regions
3. SADH mean, channel 1, mean 4x4 regions
4. SADH correlation, channel 1, 16x16 region
5. Cloud top temperature
6. SADH angular second moment, channel 1, mean 4x4 regions
7. GLDV angular second moment, channel 1, 16x16 region
8. GLDV entropy, channel 1, 16x16 region
9. GLDV mean, channel 1, 16x16 region
10. GLDV contrast, channel 1, minimum 4x4 regions
11. Minimum channel 4
12. Median channel 4
13. Minimum channel 1
14. GLDV standard deviation, channel 4, mean 4x4 regions
15. SADH mean, channel 4, 16x16 region
16. SADH mean, channel 4, maximum 4x4 regions
17. GLDV standard deviation, channel 4, std. dev. 4x4 regions
18. SADH entropy, channel 4, standard deviation 4x4 regions
19. SADH angular second moment, channel 4, maximum 4x4 regions
20. SADH entropy, channel 4, maximum 4x4 regions
21. GLDV cluster shade, channel 4, 16x16 region
22. SADH entropy, channel 1, maximum 4x4 regions
23. Mean channel 1
24. GLDV standard deviation, channel 1, minimum 4x4 regions
25. Surface temperature
26. Multilayer cloud index
27. SADH entropy, channel 1, 16x16 regions
28. SADH mean, channel 1, minimum 4x4 regions
29. SADH cluster shade, channel 1, 16x16 region
30. Cirrus cloud fraction
31. GLDV standard deviation, channel 1, mean 4x4 regions
32. GLDV local homogeneity, channel 1, 16x16 region
33. GLDV local homogeneity, channel 1, maximum 4x4 regions
34. GLDV mean, channel 1, minimum 4x4 regions
35. GLDV contrast, channel 1, mean 4x4 regions
36. GLDV contrast, channel 1, maximum 4x4 regions
37. Range of values channel 1
38. Low cloud fraction
39. Gray level distribution, channel 4
40. Gray level distribution, channel 1
41. Run percentage, channel 1
42. Run length distribution, channel 1
43. SADH angular second moment, channel 1, maximum 4x4 regions
44. SADH entropy, channel 1, minimum 4x4 regions
45. SADH mean, channel 1, maximum 4x4 regions
46. GLDV cluster shade, channel 4, mean 4x4 regions

Table 5 (continued).

- 47. GLDV contrast, channel 4, mean 4x4 regions
- 48. GLDV entropy, channel 4, mean 4x4 regions
- 49. SADH entropy, channel 4, mean 4x4 regions
- 50. SADH angular second moment, channel 1, 16x16 region

overall accuracy associated with various feature numbers. It should be noted that with every change in the number of features, experimentation was needed to determine the best value for the "smoothing parameter" (σ). The top 12 features were found to produce the highest average overall accuracy. The average overall accuracies and the standard deviations associated with each feature number are listed in Table 6.

5. Results

The top twelve features (see Table 5) were used as the input nodes for the PNN. Notice that they are comprised of 8 textural, 2 spectral (channel 4 minimum and median), and 2 physical (cloud albedo and temperature) measures. The remaining layers of the PNN included the following: 13 (number of features + 1) nodes in the normalizing layer; 410 nodes (number of training samples) in the pattern layer; 10 nodes (number of classes) in the summation layer; and 10 nodes (number of classes) in the output layer. An example diagram of a two class problem is shown in Figure 1.

An average overall accuracy of 85.15% with a standard deviation of 1.96% was obtained for the testing samples of the 10 data

Table 6. Average accuracies and standard deviations for the PNN classifier on 10 data sets using a varying number of features.

<u>Feature Number</u>	<u>Avg. Overall Accuracy</u>	<u>Standard Deviation</u>
5	74.70%	2.98%
10	83.15%	2.32%
11	82.95%	2.59%
12	85.15%	1.96%
13	84.60%	1.74%
14	84.05%	1.96%
15	84.30%	0.89%
16	84.00%	2.15%
17	84.70%	2.02%
18	83.85%	1.31%
19	84.20%	1.55%
20	83.35%	1.70%

sets. See Table 7. Examining the average confusion matrix (Table 8) reveals that most of the misclassifications were into classes having similar signatures. For example, cirrus misclassified as cirrostratus and vice versa; stratocumulus misclassified as stratus or cumulus; cumulus misclassified as stratocumulus; nimbostratus misclassified as cumulonimbus and vice versa. The two classes (Cs and As) with the lowest average accuracies are also the classes with the smallest number of training and testing samples. Increasing the sample size should improve the accuracy. Encouraging results occurred in four of the classes (Cc, Ns, St, and Clr) where the average accuracy of their testing samples was greater than 90%. In general, the accuracy obtained when running a PNN using the entire data set as training samples and the entire set as testing is the upper limit for any

Table 7. Average accuracies and standard deviations for 12 feature PNN classifier using 10 data sets.

<u>Class</u>	<u>Avg. Accuracy</u>	<u>Standard Deviation</u>
Ci	84.29%	3.63%
Cc	95.79%	4.15%
Cs	43.33%	16.57%
As	76.92%	8.88%
Ns	91.05%	6.10%
Sc	80.00%	9.47%
St	92.14%	5.00%
Cu	86.11%	7.05%
Cb	84.28%	9.40%
Clr	96.19%	3.01%
Overall	85.15%	1.96%

particular data set. For this study, the result of 98.52% can be considered the upper bound of the accuracy (Table 9). The three classes that have less than 100% accuracy (Cs, As, and Cb) are the classes with the smallest sample sizes.

As noted earlier, data from the four AVHRR subscenes studied here were originally used for testing a multispectral technique of classification (Neu, 1990). The overall accuracy of that method was 67.4%. However, that result did include the two additional classes of Ac and CuC, which had minimal representation in the subscenes and were not included here. The use of textural and other measures, in addition to spectral measures, provided useful information in the classification of the data by the PNN discussed here. Also, the neural network approach itself, which has been shown to be superior (Key et al., 1989; Sengupta et al., 1991), was another contributing factor in the higher accuracy

Table 8. Average (10 data sets) Confusion Matrix (%).

		Automated Classification (columns)								
		Manual Classification (rows)								
	Ci	Cc	Cs	As	Ns	Sc	St	Cu	Cb	Clr
Ci	84.3	0.6	12.6	0	0	2.5	0	0	0	0
Cc	1.6	95.8	0	2.6	0	0	0	0	0	0
Cs	51.7	2.5	43.3	0	0	0.8	1.7	0	0	0
As	0	5.4	0	76.9	3.1	3.1	7.7	0	3.8	0
Ns	0	0	0	0	91.1	0	0	0	8.9	0
Sc	0	0	0	1.9	0	80.0	6.7	8.6	2.8	0
St	0	0	1.4	0	0	4.7	92.1	1.8	0	0
Cu	0	0	0	0	0	13.3	0.6	86.1	0	0
Cb	0	0	0	1.4	11.4	2.9	0	0	84.3	0
Clr	1.9	0	1.9	0	0	0	0	0	0	96.2

(85.15%) obtained in this study.

6. Summary

With the recent success of a neural network approach to classification of land, water, and sky elements in polar scenes (Sengupta et al., 1991), an analogous investigation into nonpolar data was performed with an emphasis on cloud classification alone. Spectral, textural, and physical features were computed in order to classify 10 cloud types (including clear). Textural measures (GLDV and SADH) were calculated for 16x16 pixel regions

Table 9. Upper limit of accuracies for 12 feature PNN classifier (entire data set training and testing).

<u>Class</u>	<u>Max Accuracy</u>	<u>Sample Size</u>
Ci	100.00%	106
Cc	100.00%	57
Cs	83.78%	37
As	97.50%	40
Ns	100.00%	59
Sc	100.00%	65
St	100.00%	86
Cu	100.00%	54
Cb	95.12%	41
Clr	100.00%	65
Overall	98.52%	610

and the 16 4x4 pixel regions within the 16x16 area. The maximum, minimum, mean, and standard deviation values of the smaller "boxes" were computed and used as features. Spectral measures included the maximum, minimum, range, mean, median, mode, and standard deviation of pixel values within the 16x16 regions. Run length statistics were also computed. All of the textural measures, spectral measures, and run length statistics were calculated using visible (channel 1) and infrared (channel 4) data. Nine physical features were computed as well. These included visible cloud fraction, cloud albedo, surface temperature, cloud temperature, infrared cloud fraction, low cloud fraction, mid-level cloud fraction, cirrus cloud fraction, and multilayer cloud index. This brought the total number of features to 203.

The top 50 features that best discriminate the data were found using the Bhattacharya Class Separability Index and a

Sequential Forward Selection method. Of these 50, the top 12 were found to produce the highest classification accuracy using the PNN. These features, which included spectral, textural, and physical measures, produced an average overall accuracy of 85.15%, with a standard deviation of 1.96%. The two classes (Cs and As) where most of the error was found were also the least represented classes in the data set. Test samples in the Cc, Ns, St, and Clr classes were all classified with an average accuracy of greater than 90%. Higher accuracies were obtained in the study of this classification method compared with a multispectral technique used on the same images (Neu, 1990). A comparison of the sample sizes and class accuracies for the two studies is presented in Table 10.

Although preliminary, the results presented here are very encouraging. The next step involves the collection of more expertly labeled data to add to the existing set. The goal is to meet the accepted minimum requirement of sample size per class. A new validation of the classifier can then be performed on 100 data sets created using a "bootstrap" strategy of replacement samples. This method allows for the selection of a sample more than once to be a training sample in the same data set (a more complete random selection). Subsequent research must also include classifications using polar scenes. Whether the accuracy obtained here will extend to a global cloud data set is unknown;

Table 10. Class accuracies and sample testing sizes of the PNN classifier and a multispectral (MS) technique used on the same AVHRR images.

<u>Class</u>	<u>PNN Testing Sample Size</u>	<u>MS Testing Sample Size</u>	<u>PNN Accuracy</u>	<u>MS Accuracy</u>
Ci	35	27	84.3	81.5
Cc	19	9	95.8	66.7
Cs	12	12	43.3	75.0
As	13	12	76.9	58.3
Ns	19	11	91.1	54.5
Sc	21	14	80.0	57.1
St	28	23	92.1	39.1
Cu	18	34	86.1	73.5
Cb	14	14	84.3	50.0
Clr	21	18	96.2	94.4
Ac	--	3	--	33.3
CuC	--	10	--	90.0
Overall	200	187	85.2	67.4

it is possible that including polar scenes will diminish the PNN accuracy and require separate PNN classifiers.

REFERENCES

- Chen, D.W., S.K. Sengupta and R.M. Welch, 1989: Cloud field classification based upon high spatial resolution textural features. Part 2: Simplified vector approaches. J. Geophys. Res., 94, 14749-14765.
- Connors, R.W., and C.A. Harlow, 1980: A theoretical comparison of texture algorithms. IEEE Trans. Pattern Anal. Mach. Intell., PAMI-2, 204-222.
- Crosiar, C., K. Richardson and G. Haugen, 1990: Tactical environmental support system [TESS(3)] satellite cloud analysis. Proc. Oceans 90 Conf., Washington, D.C., 428-432.
- Devijver, P.A., and J. Kittler, 1982: Pattern Recognition: A Statistical Approach. Prentice Hall, Englewood Cliffs, NJ.
- Ebert, E., 1987: A pattern recognition technique for distinguishing surface and cloud types in the polar regions. J. Climate Appl. Meteor., 26, 1412-1427.
- Ebert, E., 1989: Analysis of polar clouds from satellite imagery using pattern recognition and a statistical cloud analysis scheme. J. Appl. Meteor., 28, 382-399.
- Garand, L., 1988: Automated recognition of oceanic cloud patterns. Part 1: Methodology and application to cloud climatology. J. Climate, 1, 20-39.
- Goroch, A.K., and R.M. Welch, 1989: Cloud classification of DMSP visible and IR imagery using physical and textural measures. Proc. CIDOS, Monterey, CA, Science and Technology Corp., 101 Research Dr., Hampton, VA 23666.
- Haralick, R.M., 1979: Statistical and structural approaches to texture. Proc. IEEE, 67, 786-804.
- Jurkevics, A., R. Titus and J. Clark, 1990: Environmental database for the naval environmental operational nowcasting system. Proc. 6th International Conf. on Interactive Info. and Processing Systems for Meteor., Oceanography, and Hydrology, American Meteorological Society, 45 Beacon St., Boston, MA 02108, 80-83.
- Key, J., J.A. Maslanik and A.J. Schweiger, 1989: Classification of merged AVHRR and SMMR arctic data with neural networks. Photogrammetric Engineering and Rem. Sens., 55, 1331-1338.

- Key, J., 1990: Cloud cover analysis with arctic AVHRR data. Part 2: Classification with spectral and textural measures. J. Geophys. Res., 95, 7661-7675.
- Lee, J., R. Weger, S.K. Sengupta and R.M. Welch, 1990: A neural network approach to cloud classification. IEEE Trans. Geosci. and Rem. Sens., 28, 846-855.
- Neu, T.J., 1990: Evaluation of generalized thresholds in an objective multispectral satellite cloud analysis. Master's thesis, Naval Postgraduate School, Monterey, CA 93943, 51 pp.
- Research Systems, Inc., 1990: Interactive Data Language, Version 2.0, Edition of July 24, 1990, 777 29th St., Suite 302, Boulder, CO 80303, 602 pp.
- Sengupta, S.K., P. Rabindra, N. Rangaraj and R.M. Welch, 1991: Polar cloud classification using AVHRR imagery: A neural network approach with bootstrap validation. Proc. CIDOS, Los Angeles, CA, Science and Technology Corp., 101 Research Dr., Hampton, VA 23666.
- Specht, D.F., 1990: Probabilistic neural networks. Neural Networks, 3, 109-118.
- Welch, R.M., M.S. Navar and S.K. Sengupta, 1989: The effect of spatial resolution upon texture-based cloud field classifications. J. Geophys. Res., 94, 14767-14781.
- Welch, R.M., K.S. Kuo and S.K. Sengupta, 1990: Cloud and surface textural features in polar regions. IEEE Trans. Geosci. and Rem. Sens., 28, 520-528.

DISTRIBUTION

NOARL
ATTN: CODE 104
JCSSC, MS 39529-5004

CHIEF OF NAVAL OPERATIONS
ATTN: OP-096, OP-0961B
U.S. NAVAL OBSERVATORY
WASHINGTON, DC 20392-1800

NOARL
ATTN: CODE 125L (10)
JCSSC, MS 39529-5004

NOARL
ATTN: CODE 125P
JCSSC, MS 39529-5004

NOARL
ATTN: CODE 300
JCSSC, MS 39529-5004

OFFICE OF NAVAL RESEARCH
ATTN: CODE 10
800 N. QUINCY ST.
ARLINGTON, VA 22217-5000

DIRECTOR
WOODS HOLE OCEANOGRAPHIC INST.
P.O. BOX 32
WOODS HOLE, MA 02543

UNIVERSITY OF CALIFORNIA
SCRIPPS INST. OF OCEANOGRAPHY
BOX 6049
SAN DIEGO, CA 92106

OFFICE OF NAVAL TECHNOLOGY
ATTN: DR. P. SELWYN, CODE 20
800 N. QUINCY ST.
ARLINGTON, VA 22217-5000

OFFICE OF NAVAL TECHNOLOGY
DR. M. BRISCDE, CODE 228
800 N. QUINCY ST.
ARLINGTON, VA 22217-5000

OFFICE OF NAVAL RESEARCH
ATTN: CODE 12
800 N. QUINCY ST.
ARLINGTON, VA 22217-5000

OFFICE OF NAVAL RESEARCH
DR. E. SILVA, CODE 10D/10P
800 N. QUINCY ST.
ARLINGTON, VA 22217-5000

OFFICE OF NAVAL RESEARCH
ATTN: HEAD, OCEAN SCIENCES DIV
CODE 1122
ARLINGTON, VA 22217-5000

OFFICER IN CHARGE
NAVOCEANCOMDET
AFGWC
OFFUTT AFB, NE 68113

NOARL
ATTN: A. PRESSMAN, CODE 321
JCSSC, MS 39529-5004

COMNAVOCEANCOM
ATTN: CODE N5
JCSSC, MS 39529-5000

U.S. NAVAL ACADEMY
ATTN: LIBRARY REPORTS
ANNAPOLIS, MD 21402

U.S. NAVAL ACADEMY
ATTN: OCEANOGRAPHY DEPT.
ANNAPOLIS, MD 21402

NAVAL POSTGRADUATE SCHOOL
ATTN: CODE MR
MONTEREY, CA 93943-5000

NAVAL POSTGRADUATE SCHOOL
ATTN: CODE OC
MONTEREY, CA 93943-5000

NAVAL POSTGRADUATE SCHOOL
ATTN: 0142 (LIBRARY)
MONTEREY, CA 93943-5002

NAVAIRSYSCOM
ATTN: CODE 526W
WASHINGTON, DC 20361-0001

SPAWARSYSCOM
ATTN: CODE 312
NAT. CTR. #1
WASHINGTON, DC 20363-5100

SPAWARSYSCOM
ATTN: CODE PMW-141
NAT. CTR. #1
WASHINGTON, DC 20363-5100

PACMISTESTCEN
ATTN: GEOPHYSICS OFFICER
PT. MUGU, CA 93042

AFGWC/DAPL
ATTN: TECH. LIBRARY
OFFUTT AFB, NE 68113

3 WW/DN
OFFUTT AFB, NE 68113

AFGL/LY
ATTN: MET. OFFICER
HANSCOM AFB, MA 01731

USAFETAC/TS
ATTN: TECH. LIBRARY
SCOTT AFB, IL 62225

COMMANDING OFFICER
U.S. ARMY RESEARCH OFFICE
ATTN: GEOPHYSICS DIV.
P.O. BOX 12211
RESEARCH TRIANGLE PARK, NC
27709

COMMANDER/DIRECTOR
ASL, WHITE SANDS
ATTN: SLCAS-AE
WSMR, NM 88002-5501

NOAA-NESDIS LIAISON
ATTN: CODE SC2
NASA-JOHNSON SPACE CENTER
HOUSTON, TX 77058

DIRECTOR
NATIONAL EARTH SAT. SERV/SEL
FB-4, S321B
SUITLAND, MD 20233

OCEANOGRAPHIC SERVICES DIV.
NOAA
6010 EXECUTIVE BLVD.
ROCKVILLE, MD 20852

NATIONAL WEATHER SERVICE
WORLD WEATHER BLDG., RM 307
5200 AUTH ROAD
CAMP SPRINGS, MD 20023

DIRECTOR
NATIONAL SEVERE STORMS LAB
1313 HALLEY CIRCLE
NORMAN, OK 73069

CHIEF
MESOSCALE APPLICATIONS BRANCH
NATIONAL EARTH SAT. SERV.
1225 W. DAYTON
MADISON, WI 53562

DIRECTOR
TECHNIQUES DEVELOPMENT LAB
GRAMAX BLDG.
8060 13TH ST.
SILVER SPRING, MD 20910

DIRECTOR
NATIONAL WEATHER SERVICE
GRAMAX BLDG.
8060 13TH ST.
SILVER SPRING, MD 20910

LIBRARY ACQUISITIONS
NCAR, P.O BOX 3000
BOULDER, CO 80307

HEAD, ATMOS. SCIENCES DIV.
NATIONAL SCIENCE FOUNDATION
1800 G STREET, NW
WASHINGTON, DC 20550

EXECUTIVE SECRETARY, CAO
SUBCOMMITTEE ON ATMOS. SCI.
NATIONAL SCIENCE FOUNDATION
RM. 510, 1800 G. STREET, NW
WASHINGTON, DC 20550

DR. MARVIN DICKERSON
L-262, LLNL
P.O BOX 808
LIVERMORE, CA 94550

COLORADO STATE UNIVERSITY
ATMOSPHERIC SCIENCES DEPT.
ATTN: DR. WILLIAM GRAY
FORT COLLINS, CO 80523

CHAIRMAN
INSTITUTE OF ATMOS. PHYSICS
UNIV. OF ARIZONA
TUSCON, AZ 85721

SCRIPPS INSTITUTION OF
OCEANOGRAPHY, LIBRARY
DOCUMENTS/REPORTS SECTION
LA JOLLA, CA 92037

ATMOSPHERIC SCIENCES DEPT.
UCLA
405 HILGARD AVE.
LOS ANGELES, CA 90024

WOODS HOLE OCEANO. INST.
DOCUMENT LIBRARY LO-206
WOODS HOLE, MA 02543

CHAIRMAN, METEOROLOGY DEPT.
UNIVERSITY OF OKLAHOMA
NORMAN, OK 73069

CHAIRMAN, METEOROLOGY DEPT.
CALIFORNIA STATE UNIVERSITY
SAN JOSE, CA 95192

COLORADO STATE UNIVERSITY
ATTN: ATMOSPHERIC SCI. DEPT.
FT. COLLINS, CO 80523

NATIONAL CENTER FOR ATMOS.
RSCH., LIBRARY ACQUISITIONS
P.O. BOX 3000
BOULDER, CO 80302

UNIVERSITY OF WASHINGTON
ATMOSPHERIC SCIENCES DEPT.
SEATTLE, WA 98195

CHAIRMAN, METEOROLOGY DEPT.
PENNSYLVANIA STATE UNIV.
503 WALKER BLDG.
UNIVERSITY PARK, PA 16802

UNIVERSITY OF HAWAII
ATTN: METEOROLOGY DEPT.
2525 CORREA ROAD
HONOLULU, HI 96822

ATMOSPHERIC SCIENCES DEPT.
OREGON STATE UNIVERSITY
CORVALLIS, OR 97331

UNIVERSITY OF MARYLAND
METEOROLOGY DEPT.
COLLEGE PARK, MD 20742

CHAIRMAN
METEOROLOGY DEPT.
MASSACHUSETTS INSTITUTE OF
TECHNOLOGY
CAMBRIDGE, MA 02139

CHAIRMAN, METEOROLOGY DEPT.
UNIVERSITY OF UTAH
SAL LAKE CITY, UT 84112

TEXAS A&M UNIVERSITY
METEOROLOGY DEPT.
COLLEGE STATION, TX 77843

ATMOSPHERIC SCIENCES CENTER
DESERT RESEARCH INSTITUTE
P.O. BOX 60220
RENO, NV 89506

ATMOSPHERIC SCI. RSCH. CENTER
NEW YORK STATE UNIV.
1400 WASHINGTON AVE.
ALBANY, NY 12222

THE EXECUTIVE DIRECTOR
AMERICAN METEORO. SOCIETY
45 BEACON ST.
BOSTON, MA 02108

DIRECTOR
WORLD METEOROLOGICAL
ORGANIZATION
CASE POSTALE #5, CH-1211
GENEVA, SWITZERLAND

BUREAU OF METEOROLOGY
ATTN: SROD, NMC
BOX 1289K, GPO MELBOURNE
VICTORIA 3001, AUSTRALIA

LIBRARY, AUSTRALIAN NUMERICAL
METEOROLOGY RESEARCH CENTER
P.O. BOX 5089A
MELBOURNE, VICTORIA, 3001
AUSTRALIA

CHAIRMAN, METEOROLOGY DEPT.
MCGILL UNIVERSITY
805 SHERBROOKE ST., W.
MONTREAL, QUEBEC
CANADA H3A 2K6

DEPARTMENT OF METEOROLOGY
UNIVERSITY OF READING
2 EARLYGATE, WHITEKNIGHTS
READING RG6 2AU
ENGLAND

METEOROLOGISCHES INSTITUT
DER UNIVERSITAT KOELN
5000 KOELNWETERDIENST
FEDERAL REPUBLIC OF GERMANY

EUROPEAN SPACE OPERATIONS
ATTN: DR. J. MORGAN, METEO.
SAT. DATA, MANAGEMENT DEPT.
R. BOSCH STR 5 D61 DARMSTADT
FEDERAL REPUBLIC OF GERMANY

INSTITUT FUR METEOROLOGIE
J. GUTENBERG UNIVERSITAT
ATTN: DR. R. JAENICKE
D-65 MAINZ
FEDERAL REPUBLIC OF GERMANY

REPORT DOCUMENTATION PAGE

Form Approved
OMB No. 0704-0188

Public reporting burden for this collection of information is estimated to average 1 hour per response, including the time for reviewing instructions, searching existing data sources, gathering and maintaining the data needed, and completing and reviewing the collection of information. Send comments regarding this burden estimate or any other aspect of this collection of information, including suggestions for reducing this burden, to Washington Headquarters Services, Directorate for Information Operations and Reports, 1215 Jefferson Davis Highway, Suite 1204, Arlington, VA 22202-4302, and to the Office of Management and Budget, Paperwork Reduction Project (0704-0188), Washington, DC 20503.

1. Agency Use Only (Leave blank).		2. Report Date. October 1991	3. Report Type and Dates Covered. Final
4. Title and Subtitle. A Probabilistic Neural Network Approach to Cloud Classification		5. Funding Numbers. Program Element No. 62435N Project No. RM35G82 Task No. 4 Accession No. DN651750	
6. Author(s). R.L. Bankert, P. Rabindra*, S.K. Sengupta**		7. Performing Organization Name(s) and Address(es). Naval Oceanographic and Atmospheric Research Laboratory Atmospheric Directorate Monterey, CA 93943-5006	
8. Performing Organization Report Number. NOARL Technical Note 173		9. Sponsoring/Monitoring Agency Name(s) and Address(es). Office of Naval Technology (Code 22) 800 N. Quincy St. Arlington, VA 22217	
10. Sponsoring/Monitoring Agency Report Number. NOARL Technical Note 173		11. Supplementary Notes. * P. Rabindra, UCAR visiting student ** S.K. Sengupta, UCAR visiting senior scientist	
12a. Distribution/Availability Statement. Approved for public release; distribution is unlimited.		12b. Distribution Code.	
13. Abstract (Maximum 200 words). Automated satellite image interpretation would be useful in many forecasting operations. One aspect of that interpretation, cloud classification, is examined. Ten classes, composed of low, middle, high, and precipitation cloud types plus clear, are used as output nodes in a Probabilistic Neural Network (PNN) approach to classification of data using four Advanced Very High Resolution Radiometer (AVHRR) subscenes. Input to the neural network consists of 12 features that include a mixture of spectral, textural, and physical measures. These measures are selected, using a feature selection routine, from a collection of over 200 features. An overall accuracy of 85.25% is the result. Five classes have agreement of 90% or better. The three classes with the poorest accuracies were presented to the classifier with the smallest sample sizes. An increase in the number of samples should increase the accuracy of the classifier.			
14. Subject Terms. Neural network Cloud classification Textures		15. Number of Pages. 36	
16. Price Code.		17. Security Classification of Report. UNCLASSIFIED	
18. Security Classification of This Page. UNCLASSIFIED		19. Security Classification of Abstract. UNCLASSIFIED	
20. Limitation of Abstract. None			